Parameter Uncertainty in Shallow Rainfall-triggered Landslide Modeling at Basin Scale: A Probabilistic Approach

Available online at www.sciencedirect.com

SciVerse ScienceDirect

Procedia Earth and Planetary Science00 (2014) 000–000

Procedia
Earth and Planetary Science

www.elsevier.com/locate/procedia

The Third Italian Workshop on Landslides

Parameter Uncertainty in Shallow Rainfall-Triggered Landslide Modeling at Basin Scale: a Probabilistic Approach

E. Arnone[a,b]*, Y.G. Dialynas[b], L.V. Noto[a], R.L. Bras[b]

[a]*Dipartimento di Ingegneria Civile, Ambientale, Aerospaziale, dei Materiali, Universita' degli Studi di Palermo, Viale delle Scienze ed. 8, Palermo, 90128, Italy*

[b]*School of Civil and Environmental Engineering, Georgia Institute of Technology, 790 Atlantic Drive, Atlanta, GA, 30332,USA*

Abstract

This study proposes a methodology to account for the uncertainty of hydrological and mechanical parameters in coupled distributed hydrological-stability models for shallow landslide assessment. A probabilistic approach was implemented in an existing eco-hydrological and landslide model by randomizing soil cohesion, friction angle and soil retention parameters. The model estimates the probability of failure through an assumed theoretical Factor of Safety (FS) distribution, conditioned on soil moisture content. The time-dependent and spatially distributed FS statistics are approximated by the First Order Second Moment (FOSM) method. The model was applied to the Rio Mameyes Basin, located in the Luquillo Experimental Forest in Puerto Rico.

Selection and peer-review under responsibility of Dipartimento di Ingegneria Civile, Design, Edilizia e Ambiente, Seconda Universit di Napoli.

Keywords: Rainfall-Triggered Landslides; Hydrological Modeling; Uncertainty; Probability;

1. Introduction

The use of coupled distributed hydrological-stability models for shallow landslide hazard assessment at catchment scale is common in the literature. The practice is to utilize the basin hydrological response, evaluated in terms of soil moisture and groundwater fields, to assess a spatially distributed Factor of Safety (FS) by using the

* Corresponding author. Tel.: +39-091-23896544; fax: +39-091-427121.
E-mail address: elisa.arnone@unipa.it

1878-5220
Selection and peer-review under responsibility of Dipartimento di Ingegneria Civile, Design, Edilizia e Ambiente, Seconda Universit di Napoli.

infinite slope model [1-5]. Mechanical and hydrological soil properties play a crucial role in such an evaluation, and the importance of appropriately modeling soil water dynamics has been clearly demonstrated in some studies [6, 7].

The inability to fully characterize hydrological and geotechnical behavior of soil may have a significant impact on model results. Spatial variation of parameters is difficult to describe accurately, and measurement errors can also increase the natural variability of parameters. To account for this uncertainty, FS can be computed within a probabilistic framework, by considering soil parameters as random variables and thus, assigning them probability distributions instead of deterministic values. This practice has received considerable attention in the geotechnical engineering literature, which proposes different methodologies for modeling and analyzing the uncertainty related to the shear strength parameters (i.e. soil cohesion and friction angle) at hillslope scale [8-10]. Based on similar approaches, some studies have been conducted for basin scale applications within coupled hydrological-stability models [5, 11-13]; in such applications, the probability of FS, conditioned to the soil moisture, is dynamically estimated across the basin, whereas the probability distributions of the shear strength parameters are time independent. However, the uncertainty of soil hydrological properties, which may be predominant in case of unsaturated conditions, is still neglected in most published literature. In particular, soil retention curve parameters are the most significant in determining the contribution of the soil matric suction to the equilibrium.

The probability distribution of FS can be derived numerically, analytically or through analytical approximations. The Monte Carlo simulation method uses independent sets of soil properties, generated through a priori assigned probability distributions [8, 10] at fixed topographic (i.e. slope) and hydrological (i.e. soil moisture) conditions to obtain a solution. However, such an approach may have significant computational cost for basin scale applications, since the above mentioned conditions change in time and space. The FS probability distribution can be analytically derived in the case where solely geotechnical parameters (i.e., cohesion and friction angle) are considered as random variables (e.g., for saturated conditions) and the infinite slope model is used for the slope stability analysis [8, 10]. When the soil retention curve parameters are also assumed to be random (e.g. for unsaturated conditions), analytical derivation of FS distribution is not tractable [8, 10]. In this case, the First Order Second Moment (FOSM) method [14] is commonly used to estimate analytical approximations of the spatio-temporal FS statistics (i.e. mean and variance), to finally fit a theoretical probability distribution for FS and estimate the spatio-temporal dynamics of probability of failure.

In order to systematically account for the parameter uncertainty, we propose a probabilistic approach for coupled distributed hydrological-stability models based on the FOSM method, which was implemented in the tRIBS-VEGGIE (*Triangulated Irregular Network (TIN)-based Real-time Integrated Basin Simulator - VEGetation Generator for Interactive Evolution*) - Landslide module [7]. The proposed methodology was applied to the Rio Mameyes Basin, located in the Luquillo Experimental Forest in Puerto Rico, where previous landslide analyses have been carried out. The main purpose of the application is to demonstrate the model capabilities and highlight further possible improvements.

2. Methodology

2.1. Model Overview

tRIBS-VEGGIE-landslide module [7] is built upon the eco-hydrological model tRIBS-VEGGIE, which consists of a spatially distributed physically based hydrological model coupled to a model of plant physiology and spatial dynamics [15]. Basin hydrological response is simulated on an irregular spatial mesh which allows for the use of variable computational elements to describe the basin topography, by increasing the accuracy only in the most critical areas of the basin [16]. The model explicitly considers the spatial variability in land-surface descriptors and the corresponding moisture dynamics, stressing the role of topography in lateral redistribution. The infiltration module is responsible of the moisture fields computation and is based on a numerical approximation of the one dimensional Richards' equation [17]. The dynamics of each computational element are simulated separately, but spatial dependencies are introduced by considering the surface and subsurface moisture transfers among the

elements along the direction of steepest descent, based upon the unsaturated hydraulic conductivity of the receiving cell. The soil retention and the unsaturated hydraulic conductivity are related to soil-moisture content through the Brooks and Corey [18] (BC) parameterization scheme [19], as a function of saturated hydraulic conductivity in the normal to the soil surface direction, air entry bubbling pressure, and pore-size distribution index. Vegetation affects the soil moisture dynamics mainly by extracting soil water for the purposes of transpiration, considered as soil moisture sink.

The landslide module is based on the assessment of the Factor of Safety (FS) by applying the limit equilibrium analysis within the infinite slope model. The model dynamically computes FS across the study area through the following equation [7]:

$$FS = \frac{c'}{\gamma_s z_n \sin\alpha} + \frac{\tan\phi}{\tan\alpha} + \frac{\gamma_w \psi_b}{\gamma_s z_n} \cdot \left(\frac{\theta_w - \theta_r}{\theta_s - \theta_r} \right)^{1-\frac{1}{\lambda}} \cdot \frac{\tan\phi}{\sin\alpha} \tag{1}$$

where *c'* is the effective soil cohesion, γ_s is the total unit weight of soil (varying with soil moisture), γ_w is the water unit weight, z_n is the soil depth measured along the normal direction to the slope; α is the slope angle, ϕ is the soil friction angle, ψ_b is the air entry bubbling pressure, λ is the pore-size distribution index, θ_w is the volumetric water content, and θ_r and θ_s are the residual and saturated soil moisture contents, respectively. ψ_b, λ, θ_r and θ_s are the BC [18] parameters used to model the soil retention curve. As a result of the multi-layer representation of soil moisture within tRIBS-VEGGIE, the final product of the module is a spatially distributed vertical dynamic FS profile that takes into account the local moisture and soil conditions within each computational element.

2.2. FS distribution

The implemented probabilistic framework for FS includes the analytical approximation of FS statistical properties (i.e., mean and variance), variant in time and space, by using the FOSM method, and fitting a theoretical probability distribution function for FS (see section 3.3).

The FOSM method applies the first order Taylor expansion, from which first and second order moments are derived. More precisely, if we consider a function of several random variables, $X_1,\ldots,X_n$: $Y=y(X_1,\ldots,X_n)$, taking the Taylor series expansion about the mean $\mu_{X1}, \ldots, \mu_{Xn}$, and retaining terms up to first order leads to the following expressions of first and second moments [20]:

$$E(Y) = y(\mu_{x1},\ldots,\mu_{xn}) \tag{2}$$

$$Var(Y) = E\left[\left(\sum_{i=1}^{n} (X_i - \mu_{xi})^2 \frac{\partial y}{\partial X_i} \right)^2 \right] = \sum_{i=1}^{n} \left(\frac{\partial y}{\partial X_i} \right)^2 Var(X_i) + 2 \sum_{i=1}^{n} \sum_{j=1}^{n-1} \left(\frac{\partial y}{\partial X_i} \right) \left(\frac{\partial y}{\partial X_j} \right) Cov(X_i, X_j) \tag{3}$$

where *E(Y)* and *Var(Y)* are the mean and the variance, respectively, of the dependent variable *Y*, *n* is the number of random variables, $Var(X_i)$ is the variance of random variables X_i, and $Cov(X_i, X_j)$ is the covariance between X_i and X_j, which is known given the corresponding correlation coefficient, ρ_{XiXj}. Analytical expressions of *y* derivatives with respect to the random variables require that *y* is continuously differentiable.

In this analysis, the soil parameters *c'*, $\tan\phi$, θ_r, θ_s, ψ_b, and λ of the FS formulation (Eq.1) are assumed as random variables. Eq. 1 is thus continuously differentiable with respect to each random variable. Given the marginal statistics of the above mentioned parameters it is possible to estimate the temporally and spatially variant mean and variance of FS, i.e., *E[FS]* and *Var(FS)*, respectively. Then, an assumed theoretical distribution function is used to estimate the probability of FS. At this point, Monte Carlo experiments are required to identify the best fit theoretical distribution of FS (see Section 3.3).

Under saturated conditions, it is possible to obtain the analytical solution of the FS probability distribution and the use of the FOSM method is not necessary. In fact, the soil retention curve parameters do not directly affect the FS formulation, which results in a linear function of random variables c' and $\tan\phi$. In this case, the distribution of FS can be analytically derived, assuming that cohesion and friction angle are uncorrelated normal random variables [5, 8, 10]. Consequently, FS follows a normal distribution, and the associated statistics (i.e., mean and variance of FS) are estimated analytically.

The procedure has been implemented into the tRIBS-VEGGIE-Landslide model to dynamically evaluate the probability of landslide occurrence. For each timestep and at each layer (i) of the soil column cell, the model computes the probability that FS is equal or lower than 1 (implying failure, PrF_i) assuming independent events among different layers. The probability that a landslide occurs somewhere in the soil column cell is evaluated as the probability of the union of events for the entire column ($PrFC$). The most probable depth of failure or, equivalently, the probability that the plane of failure at the given column is located at a certain depth, is given by the joint probability of FS being equal or lower than 1 at a certain depth, while there is no failure above ($PrPF_i$). As a result, the model is capable of providing the spatial distribution of $PrFC$, and the maximum value of $PrPF_i$ along with the corresponding depth, which constitutes the most probable landslide depth. Moreover, the model allows for the visualization, at any selected cell, of the temporal and vertical profile of PrF_i and $PrPF_i$.

3. Case Study

3.1. Basin Description

The Rio Mameyes basin, located in the Luquillo Experimental forest (LEF) in the island of Puerto Rico, was selected for testing the model. The LEF is part of both the Long-Term Ecological Research (LTER) and the Critical Zone Observatory (CZO) networks and has been a focal point for studies of landslide impacts on ecology, geomorphology, biology, disturbance and recovery of vegetation [21-24].The basin has been modeled for dynamic landslide analysis previously by Lepore et al. [7] using the tRIBS-VEGGIE-Landside model.

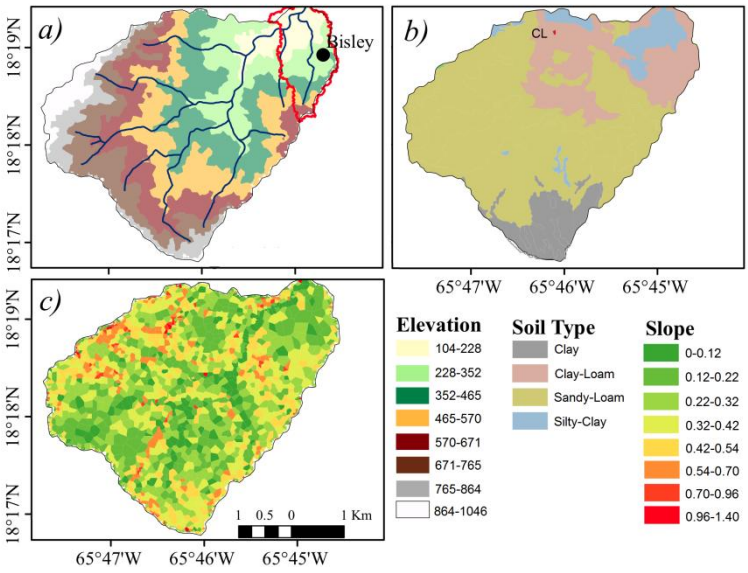

Fig. 1. Major characteristics of the Rio Mameyes Basin: (a) Digital Elevation Model, drainage system and meteorological station. The red polygon delineates the area where model validation was conducted based on soil moisture data (Lepore et al. [7]); (b) soil type distribution and Clay-Loam element selected for the analysis; (c) slope distribution. Modified from Lepore et al. [7].

The basin has an area of 16.7 km^2 and it is characterized by a strong gradient in elevation, which ranges from 104.2 m to 1046 m across a horizontal distance of 3 km (see Digital Elevation Model, DEM, in Fig.1a). Because of the strong gradient in elevation, meteorological variables (e.g. rainfall and temperature) vary consistently throughout the basin [25, 26]. The mean annual precipitation (MAP) varies from approximately 3000 mm, measured at an elevation of 352 m (Bisley Tower), to 5000 mm at higher elevations [27] resulting in one of the wettest basins on the island. The analysis of the slope distribution (see Fig. 1d) reveals 10% of the basin area being characterized by slopes greater than 30°, and 30% of the basin area with slopes greater than 25°. In terms of vegetation, the Luquillo forest is characterized by a combination of lower montane wet tropical, wet subtropical and rain forest [28]. The predominant vegetation type of the basin is the Tabonuco forest (*Dacryodes excelsa*), present in the wet subtropical and subtropical rain forest life zones, typically within the 150-600 m elevation range. Further details on description of the area and available data are provided by Lepore et al. [7].

3.2. Data and Model Parameters

The model inputs used in this study (i.e., meteorological forcing, soil properties, and model parameters) are the same as defined in Lepore et al. [7]. In particular, the hydrological soil properties have been set and tuned through a validation/confirmation procedure based on soil moisture data. Final values of the main soil parameters are given in Table 1. Moreover, the case of anisotropy ratio (i.e., the ratio of the saturated hydraulic conductivities in the directions parallel to the slope and normal to the slope) equal to 100 is analyzed. Meteorological data (wind speed and direction, air temperature, cloud cover, relative humidity, rainfall, incoming shortwave radiation) are obtained from the Bisley meteorological tower (lat. 18.31, long. 65.74, 352 m) (see Fig. 1a), which has been working continuously since 2002, with the exception of brief interruptions. In particular, the model was forced using a continuous series for the year 2008, during which a significant rainfall event was recorded between the 27th and 28th April, 2008 with a peak rainfall intensity of 100 mm/hr.

Table 1.Hydrological and mechanical soil properties and their statistics.

Parameter	Description	Units	Clay – Loam	Sandy – Loam	Silty - Clay	Clay
K_s	Saturated hydraulic conductivity	[mm/hr]	50.0	50.0	50.0	10.0
$\mu_{\theta S}$	Mean of saturated soil moisture, θ_S	[mm^3/mm^3]	0.56	0.55	0.55	0.53
$\mu_{\theta R}$	Mean of residual soil moisture, θ_R	[mm^3/mm^3]	0.075	0.041	0.051	0.09
μ_{λ}	Mean of pore-size distribution index, λ	[-]	0.200	0.322	0.127	0.130
$\mu_{\psi b}$	Mean of air entry bubbling pressure, ψ_b	[mm]	-250	-150	-340	-370
$\mu_{c'}$	Mean of soil effective cohesion, c'	[N/m^2]	3000	3000	3000	3000
μ_{ϕ}	Mean of soil friction angle, ϕ	[°]	25	25	25	25
$\sigma_{c'}$	Standard deviation of c'	[N/m^2]	1200	1200	1200	1200
σ_{ϕ}	Standard deviation of ϕ	[°]	2.5	2.5	2.5	2.5
$\sigma_{\psi b}$	Standard deviation of ψ_b	[mm]	290	210	390	600
$\sigma_{\theta S}$	Standard deviation of θ_S	[mm^3/mm^3]	0.054	0.076	0.064	0.048
$\sigma_{\theta R}$	Standard deviation of θ_R	[mm^3/mm^3]	0.007	0.004	0.022	0.011
σ_{λ}	Standard deviation of λ	[-]	0.113	0.145	0.094	0.098
$\rho_{\psi b\text{-}\theta S}$	Coefficient of correlation ψ_b-θ_S	[-]	0	0	0	-0.216
$\rho_{\psi b\text{-}\theta R}$	Coefficient of correlation ψ_b-θ_R	[-]	0.203	0	0	0.154
$\rho_{\psi b\text{-}\lambda}$	Coefficient of correlation ψ_b-λ	[-]	0.151	0.274	0	0.128
$\rho_{\theta S\text{-}\theta R}$	Coefficient of correlation θ_S-θ_R	[-]	0.307	0	0	0
$\rho_{\theta S\text{-}\lambda}$	Coefficient of correlation θ_S-λ	[-]	0.168	0	0	0
$\rho_{\theta R\text{-}\lambda}$	Coefficient of correlation θ_R-λ	[-]	0.429	0.518	0.476	0.442

Several studies have provided a comprehensive description of parameter distributions and statistical properties for different soil types belonging to the USDA soil classification system. Lumb [29] studied four typical soil formations and concluded that the Gaussian or a closely related distribution can adequately describe natural soils in terms of cohesion and friction angle, which agrees with Wu and Kraft [30], and Langejan [31]. In general, the normality assumption for *c'* and *tanϕ* has been used in several studies [5, 8, 10-12, 32, 33]. Statistical properties of geotechnical parameters are given in literature by Lumb [34], Fredlund and Dahlman [35], Schultze [36], among

others. Moreover, Matsuo and Kuroda [37] and Lumb [34] showed that cohesion and friction angle display negligible correlation, and hence statistical independence between *c* and *tanφ* has been assumed in several studies [8, 10, 38-40]. Therefore, independence between geotechnical parameters was assumed in the present study.

Statistical properties of the BC [18] soil retention parameters are given in literature as well. Brakensiek et al. [41] analysed 1,085 sets of soil retention data from reports by Rawls [42] and Holtan [43] and suggest transformations of the BC parameters that allow their characterization as normal distributions and give their statistical properties (i.e., means, variances and cross-correlation coefficients) for different soil types in the USDA soil classification. McCuen et al. [44] analysed the same data-set and provided BC parameters statistics and demonstrated the parameter variation across different soil textural classes. Rawls et al. [45] analyzed a total of 5,350 soil samples from a 1978 soil survey, and provided BC parameters marginal statistics. Carsel and Parrish [46] analysed approximately 5,700 samples from a soil database compiled by Carsel et al. [47] and provide statistics of van Genuchten [48] soil retention parameter statistics and corresponding transformations to normality. Their results were used by Meyer et al. [49], who applied parameter equivalencies to numerically derive BC parameter statistics and marginal distributions. Schaap and Leij [50] three data bases [51-53] (to a total size of 2,130 samples), and provided with Van Genuchten's (VG) soil retention parameter statistics. Flores et al. [54] used the Schaap and Leij [49] results and the same data sets to fit marginal distributions to BC parameters by transforming VG to BC parameters.

In this study, the Brakensiek et al. [41] results are used, since they provided marginal and joint statistics of the BC parameters, and suggested parameter transformations to normality (and thus, supporting the use of joint normal distribution for BC parameters) without using any VG – BC parameter equivalencies. The values of standard deviation of the residual soil moisture are, those given by McCuen et al. [44]. According to the Brakensiek et al. [41] statistical description of BC parameters, λ can reach values very close to zero. However, as $\lambda \to 0 \Rightarrow FS \to \infty$, and $dFS/d\lambda \to \infty$, which can be unacceptable since the implemented FOSM method requires $dFS/d\lambda < \infty$ and in general, may not be efficient in the presence of highly non-linear relationships. Therefore, the distribution of λ was truncated at a lower limit for λ (λ_{min}), and the corresponding statistics were computed. Values of soil parameters and statistical properties are reported in Table 1.

3.3. Monte Carlo experiments

Monte Carlo experiments were conducted to numerically derive empirical distributions of FS, with given hydrological and topographical conditions, and identify the best fit of analytical distribution functions. The empirical FS distributions were obtained for different hydrological and topographic conditions, i.e. soil depths, slope and soil moisture, and for the four soil types of the study area, i.e. clay, clay-loam, silty-clay, sandy loam. The fit of several theoretical distributions was evaluated. Here we show the comparison of three theoretical distributions (i.e., Normal, Gamma and Lognormal) against the empirical FS distribution (Fig. 2) numerically obtained for a set of values of slope, depth of failure surface and volumetric water content equal to 43°, 500 mm and 0.3 mm^3/mm^3 respectively, and for the statistical parameters reported in Table 1.

In all cases, the lognormal distribution (red line) seems to more appropriately describe the FS distribution. In particular, the lognormal better reproduces the positive skewness of the empirical FS distribution, and thus more efficiently captures the probability of failure, whereas the normal distribution tends to overestimate the occurrence of high values of FS. This is also supported by the results reported by Frattini et al. [11], who demonstrated that the lognormal function properly describes the FS distribution for different soil formations. Similar results were obtained for different hydrological and topographic conditions.

Based on the Monte Carlo experiments results, the lognormal distribution was implemented to model the FS distribution within tRIBS-VEGGIE-Landslide and evaluate the probability of failure across the basin. However, it is worth pointing out that the best fit distribution may vary for different sets of soil parameter statistics. Therefore, the results shown here are valid only for the set of parameters given in Table 1.

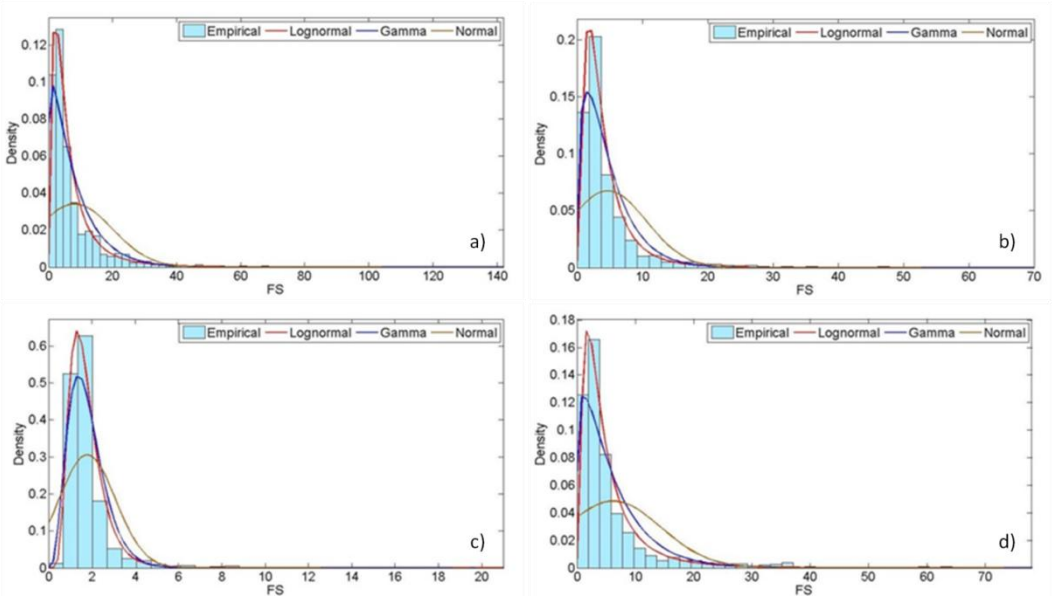

Fig. 2. Comparison between FS empirical (numerically derived) pdf, Lognormal (red), Gamma (blue), and Normal (yellow) theoretical fits for (a) clay, (b) clay loam, (c) sandy loam, and (d) silty clay. The used values of slope, depth of failure surface and volumetric water content are equal to 43°, 500 mm and 0.3 mm^3/mm^3 respectively, while the used values of statistical parameters are reported in Table 1.

3.4. Model results

In this section the results from the model application are described and discussed. As explained in section 2.2., the model output includes: the spatial distribution of the probability that failure occurs at any depth within a given element-soil column (*PrFC*), for specified maximum soil thickness; the spatial distribution of the most probable depth of failure; at selected elements and each layer, the probability that FS≤1 (PrF_i); and finally the probability that the plane of failure is located at the corresponding depth ($PrPF_i$).

Fig. 3 illustrates screenshots of *PrFC* at the time of the maximum rainfall intensity (*t1*, 103 mm/hr), and two hours later (*t2*, 24.4 mm/hr) (Fig.3a and b, respectively). The likelihood of failure occurrence is particularly high (Fig.3a, red regions) in the steepest part of the basin (see slope distribution in Fig. 1d), with 10% of the basin area resulting in a *PrFC* higher than 0.8, as depicted by the frequency distribution reported in Fig.4a. Values higher than 0.5 correspond to 19% of the basin (8.5% is between *PrFC* of 0.2 and 0.5, Fig.4a). Note that in the south-eastern region, the *PrFC* rarely reaches values less than 0.2. This part of the basin is characterized by clayey soil corresponding to higher variation coefficient of BC parameter ψ_b, which increases suction uncertainty. This leads to greater FS variance and higher uncertainty around stability, which in turn results in higher probability of failure. *PrFC* between 0.2 and 0.5 (yellow class in Fig.3a and b) characterizing 13% of total area (Fig.4a), is spread across the basin. At *t2* (Fig.3b and Fig.4a), the percentage of basin with high *PrFC* (8.8%) does not decrease significantly. The percentage of the area corresponding to *PrFC* between 0.2 and 0.5 drops to 7.5%, with a decrease in *PrFC* especially in the central and the north-eastern part of the basin. No significant changes between *t1* and *t2* are observed for clayey soils, characterized by lower soil moisture dynamics. In general, at *t2* lower values of *PrFC* are more frequent compared to *t1*, since soil moisture reduces across the basin.

Fig.3 c, d report maps of the depth of the most probable plane of failure, obtained by excluding the portion of the basin with *PrFC* lower than 0.5, at *t1* and *t2*, respectively. The corresponding relative frequency distribution is shown in Fig.4b. The most frequent depth for the former case (Fig.3c) corresponds to the range of 200-600 mm, mainly distributed in the upstream north-central part of the basin. This is followed by the range of 850-1250 mm, most of which occur in the clayey area (south-east). That is, because steeper slopes at high soil moisture conditions can be prone to failure at shallower depths. Only in a few cases (0.04 of total, see Fig.4b) the most probable plane

of failure corresponds to deeper depths. At *t2* (Fig.3d), the probability that failure is initiated at shallower depths decreases, and landslides tend to occur at deeper depths (i.e. 1250-1500 mm) with higher frequency. This can be given to soil moisture reduction at *t2*, which decreases destabilizing forces. Thus, greater soil weight is required for landslide initiation, which sets the most probable plane of failure deeper, compared to *t1*.

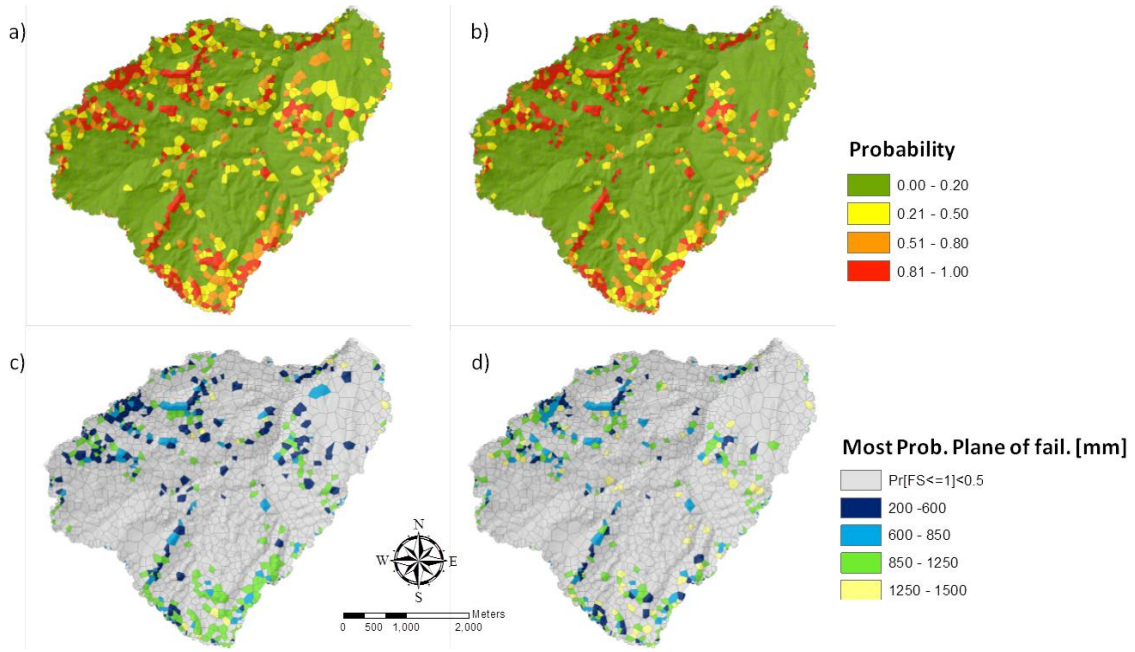

Fig. 3.Spatial distribution of *PrFC* (a) at the time of the maximum rainfall intensity (*t1*,103 mm/hr) and (b) two hours later (*t2*, 24.4 mm/hr). Spatial distribution of the corresponding depth of the most probable plane of failure (c) and (d).

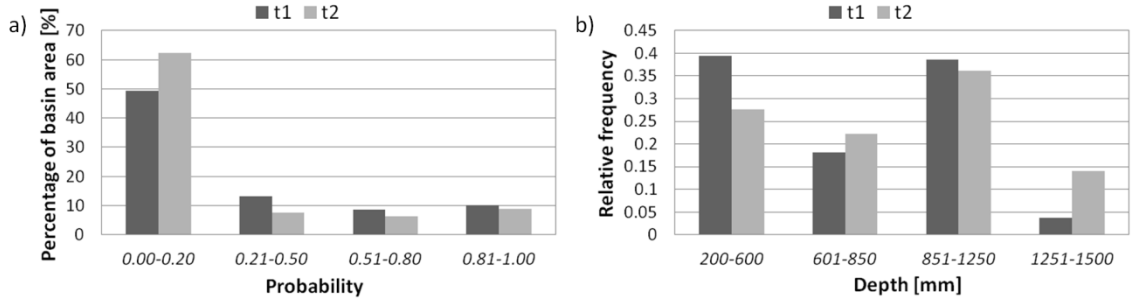

Fig. 4. (a) Frequency distribution of the probability of failure of soil column across the basin (*PrFC*); (b) frequency distribution of depth of the most probable plane of failure across the basin, for PrFC> 0.5.

The temporal evolution of landslide likelihood is analysed at element scale for a selected element within the Clay-Loam soil type (CL) with a slope of 52° (see Fig.1b). Fig.5 shows the profiles in time and depth, of soil moisture (Fig.5b), and the probability that the plane of failure at the given element is located at certain depth, *PrPFi* (Fig.5c) as a response to the rainfall forcing shown in Fig.5a. Around the rainfall peak (*t1*) higher values of soil moisture are reached at shallow depths. The green closed region in panel c depicts the peak of *PrPFi*, located between 350-450 mm, at the time of the heavy rainfall. Thus, green color (Fig.5c) indicates the area of most probable depth and time of landslide occurrence. The profile can also be interpreted as the temporally variant probability function of landslide depth, which has its maximum within the range of 300-500 mm, consistently with

the characteristics of the shallow landslides.

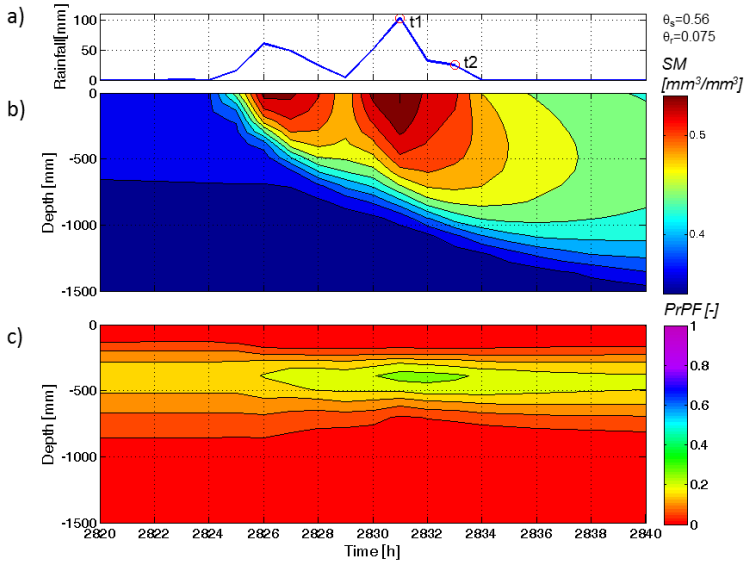

Fig. 5.Time varying model output at selected cell: (a) rainfall forcing; (b) soil moisture profile; (c) probability of plane of failure profile (i.e. probability that plane of failure at the given element is located at certain depth. Clay-Loam, slope 52°.

4. Conclusions

Natural variability of soil parameters significantly affects the hydrological and geomorphological modeling and a fully soil characterization cannot commonly be reproduced. Here we proposed a probabilistic approach for rainfall-induced landslide modeling which takes into account geotechnical and hydrological parameter uncertainty. The methodology considers soil strength and retention curve parameters as random variables, and approximations of FS statistics are estimated by means of the First Order Second Moment (FOSM) method.

The procedure was implemented into the tRIBS-VEGGIE-Landslide model and applied to the Rio Mameyes Basin, Luquillo Experimental Forest in Puerto Rico, as a demonstration of the model capabilities and required improvements. The model output provides a dynamic hazard classification of the basin in terms of probability of failure initiation conditioned on soil moisture. Moreover, the location and the timing of the most probable plane of failure are estimated by computing the joint probability of FS being less than 1 at each depth, while shallower soil layers remain stable. The use of the proposed probabilistic approach is able to reveal and quantify landslide risk at slopes assessed as stable by simpler deterministic methods.

Future developments of this work may include further investigations on soil characterization in terms of mechanical and statistical properties. A sensitivity analysis of the model to statistical parameters will improve our understanding of model behavior as soil characteristics change, along with additional Monte Carlo experiments to evaluate how the FS distribution changes with varying parameter statistics. Furthermore, future developments may also involve the analysis of the effect of the gradient in precipitation on landslide hazard evaluation, which strongly characterizes the basin under study.

Acknowledgements

This work was funded by a subcontract from the University of Pennsylvania's Luquillo Critical Zone Observatory effort, funded by the National Science Foundation. ARRA funds were utilized for the effort.

References

1. Arnone E, Noto LV, Lepore C, Bras RL. Physically-based and distributed approach to analyze rainfall-triggered landslides at watershed scale. *Geomorphology* 2011,**133**:121-131.
2. Capparelli G, Versace IP. FLaIR and SUSHI: two mathematical models for early warning of landslides induced by rainfall. *Landslides* 2010,**8**:67-79.
3. Montgomery DR, Dietrich WE. A physically based model for the topographic control on shallow landsliding. *Water Resources Research* 1994,**30**:1153-1171.
4. Rosso R, Rulli MC, Vannucchi G. A physically based model for the hydrologic control on shallow landsliding. *Water Resources Research* 2006,**42**:16.
5. Simoni S, Zanotti F, Bertoldi G, Rigon R. Modelling the probability of occurrence of shallow landslides and channelized debris flows using GEOtop-FS. *Hydrological Processes* 2008,**22**:532-545.
6. Lanni C, Rigon R, Cordan E, Tarantino A. Analysis of the effect of normal and lateral subsurface water flow on the triggering of shallow landslides with a distributed hydrological model. In: *International Conference 'Landslide Processes',France,*; 2009.
7. Lepore C, Arnone E, Noto LV, Sivandran G, Bras RL. Physically based modeling of rainfall-triggered landslides: a case study in the Luquillo forest, Puerto Rico. *Hydrol. Earth Syst. Sci.* 2013,**17**:3371-3387.
8. Abbaszadeh M, Shahriar K, Sharifzadeh M, Heydari M. Uncertainty and Reliability Analysis Applied to Slope Stability: A Case Study From Sungun Copper Mine. *Geotechnical and Geological Engineering* 2011,**29**:581-596.
9. Ray A, Baidya D. Probabilistic Analysis of a Slope Stability Problem. In: *Indian Geotechnical Conference*. Kochi; 2011. pp. K-250.
10. Abdullah I, Waleed F, Fayez A. Uncertainty and reliability analysis applied to slope stability. *Structural Safety* 2000,**22**:161-187.
11. Frattini P, Crosta G, Sosio R. Approaches for defining thresholds and return periods for rainfall-triggered shallow landslides. *Hydrological Processes* 2009,**23**:1444-1460.
12. Melchiorre C, Frattini P. Modelling probability of rainfall-induced shallow landslides in a changing climate, Otta, Central Norway. *Climatic Change* 2012,**113**:413-436.
13. Pack RT, Tarboton DG, Goodwin CN. *SINMAP, a stability index approach to terrain stability hazard mapping. SINMAP user's manual*: Terratech Consulting Ltd; 1998.
14. Benjamin JRA, Cornell CAA. *Probability, Statistics, and Decision for Civil Engineers*: McGraw-Hill Ryerson, Limited; 1970.
15. Ivanov V, Bras RL, Vivoni ER. Vegetation-Hydrology Dynamics in Complex Terrain of Semiarid Areas: II. Energy-Water Controls of Vegetation Spatio-Temporal Dynamics and Topographic Niches of Favorability. *Water Resources Research* 2008,**44**:W03430.
16. Vivoni ER, Ivanov VY, Bras RL, Entekhabi D. Generation of triangulated irregular networks based on hydrological similarity. *Journal of Hydrologic Engineering* 2004,**9**:288-302.
17. Hillel D. *Fundamentals of soil physics*: Academic Press, New York, NY, USA; 1980.
18. Brooks RH, Corey AT. Hydraulic properties pf porous media. *Hydrology Paper, Civil Engineering Dep.* 1964.
19. Sivandran G, Bras RL. Identifying the optimal spatially and temporally invariant root distribution for a semiarid environment. *Water Resources Research* 2012,**48**:W12525.
20. Maskey S, Guinot V. Improved first-order second moment method for uncertainty estimation in flood forecasting. *Hydrological Sciences Journal* 2003,**48**:183-196.
21. Myster RW, Thomlinson JR, Larsen MC. Predicting landslide vegetation in patches on landscape gradients in Puerto Rico. *Landscape Ecology* 1997,**12**:299-307.
22. Scatena FN, Lugo AE. Geomorphology, disturbance, and soil and vegetation of two subtropical wet steepland watersheds of Puerto Rico. *Geomorphology* 1995,**13**:199-213.
23. Shiels AB, West CA, Weiss L, Klawinski PD, Walker LR. Soil factors predict initial plant colonization on Puerto Rican landslides. *Plant Ecology* 2008,**195**:165-178.
24. Walker LR, Shiels AB. Post-disturbance erosion impacts carbon fluxes and plant succession on recent tropical landslides. *Plant and Soil* 2008,**313**:205-216.
25. Daly C, Helmer EH, Quinones M. Mapping the climate of Puerto Rico, Vieques and Culebra. *International Journal of Climatology* 2003,**23**:1359-1381.
26. Garcia-Martino AR, Warner GS, Scatena FN, Civco DL. Rainfall, Runoff and Elevation Relationships in the Luquillo Mountains of Puerto Rico. *Caribbean Journal of Science* 1996,**32**:413-424.
27. Lepore C, Kamal SA, Shanahan P, Bras RL. Rainfall-Induced Landslide Susceptibility Zonation of Puerto Rico. *Environmental Earth Sciences* 2012.
28. Ewel JJ, Whitmore JL. The ecological life zones of Puerto Rico and the U.S. Virgin Islands. In: Institute of Tropical forestry, Rio Piedras, Puerto Rico; 1973.
29. Lumb P. The Variability of Natural Soils. *Canadian Geotechnical Journal* 1966,**3**:74-97.
30. Wu T, Kraft L. The Probability of Foundation Safety. *Journal of the Soil Mechanics and Foundations Division* 1967,**93**:213-231.
31. Langejan A. Some aspects of the safety factor in soil mechanics considered as a problem of probability. In: *Sixt Int. Conf. Soil Mechanics and Foundation Eng*. Montreal, Quebec; 1965. pp. 500-502.
32. Rackwitz R. Reviewing probabilistic soils modelling. *Computers and Geotechnics* 2000,**26**:199-223.
33. Tobutt DC. Monte Carlo Simulation methods for slope stability. *Computers & Geosciences* 1982,**8**:199-208.
34. Lumb P. Applications of statistics in soil mechanics. In: *Soil mechanics. New Horizons*. Edited by JK L. London; 1974.
35. Fredlund DF, Dahlman AE. Statistical Geotechnical Properties of Glacial Lake Edmonton Sediments. In: *Statistics and Probability in Civil Engineering*. Edited by Press HKU. London: Oxford University Press; 1972.
36. Schultze E. Some Aspects Concerning the Application of Statistics and Probability to Foundation Structures. In: *2nd International Conference on Applications of Statistics and Probability in Soil and Structural Engineering,*. Aachen; 1975. pp. 457-494.
37. Matsuo M, Kuroda K. Probabilistic Approach to Design of Embankments. *Soils and Foundations* 1974,**14**:1-17.
38. Christian J, Ladd C, Baecher G. Reliability Applied to Slope Stability Analysis. *Journal of Geotechnical Engineering* 1994,**120**:2180-2207.

39. Dettinger M, Wilson J. First order analysis of uncertainty in numerical models of groundwater flow part: 1. Mathematical development. *Water Resources Research* 1961,**17**:149-161.
40. Yucemen MS, Tang WH, AHS. A. Long term stability of soil slopes - a reliability approach. In: *Second Int. Conf. Applications of Statistics and Probability to Soil and Structural Eng.* Aachen, Germany.; 1975.
41. Brakensiek KL, Engleman RL, Rawls WJ. Variation within texture classes of soil water parameters. *ASAE* 1981,**24**:335-339.
42. Rawls W. *Calibration of Selected Infiltration Equations for the Georgia Coastal Plain*: Agricultural Research Service, U.S. Department of Agriculture; 1976.
43. Holtan HN. *Moisture-tension Data for Selected Soils on Experimental Watersheds*: Agricultural Research Service, U.S. Department of Agriculture; 1968.
44. McCuen RH, Rawls WJ, Brakensiek DL. Statistical analysis of the Brooks-Corey and the Green-Ampt parameters across soil textures. *Water Resources Research* 1981,**17**:1005-1013.
45. Rawls WJ, Brakensiek DL, Saxton KE. Estimation of Soil Water Properties. *Transactions American Society of Agricultural Engineers, St. Joseph, MI* 1982,**25**:1316-2320.
46. Carsel RF, Parrish RS. Developing joint probability distributions of soil water retention characteristics. *Water Resources Research* 1988,**24**:755-769.
47. Carsel RF, Parrish RS, Jones RL, Hanse JL, Lamb RL. Characterizing the uncertainty of pesticide leaching in agricultural soils. *Journal of Contaminant Hydrology* 1988,**2**:111-124.
48. van Genuchten MT. A Closed-form Equation for Predicting the Hydraulic Conductivity of Unsaturated Soils1. *Soil Sci. Soc. Am. J.* 1980,**44**:892-898.
49. Meyer PD, Rockhold ML, Gee GW. *Uncertainty analyses of infiltration and subsurface flow and transport for SDMP sites*. Washington, DC: Pacific Northwest National, Laboratory, Division of Regulatory Applications, Office of Nuclear Regulatory Research, U.S. Nuclear Regulatory Commission 1997.
50. Schaap M, Leij F. Database-related accuracy and uncertainty of pedotransfer functions. *Soil Science* 1998,**163**:765-779.
51. Ahuja LR, Cassel DK, Bruce RR, Barnes BB. Evaluation of Spatial Distribution of Hydraulic Conductivity using Effective Porosity Data. *Soil Science* 1989,**148**:404-411.
52. Leij FJ, Alves W, Van Genuchten MT, Williams JR. *The UNSODA unsaturated soil hydraulic database: user's manual*: National Risk Management Research Laboratory, Office of Research and Development, U.S. Environmental Protection Agency; 1996.
53. Rawls WJ, Brakensiek DL. Prediction of Soil Water Properties for Hydrologic Modeling. In: *Watershed Management in the Eighties*. Edited by E. B. Jones aTJW. Denver, Colorado: ASCE; 1985. pp. 293-299.
54. Flores AN, Entekhabi D, Bras RL. Reproducibility of soil moisture ensembles when representing soil parameter uncertainty using a Latin Hypercube–based approach with correlation control. *Water Resources Research* 2010,**46**:W04506.